Salt-Enhanced Oxidative Addition of Iodobenzene to Pd: an Interplay Between Cation, Anion and Pd-Pd Cooperative Effects

Haosheng Liang,‡ Jordan Rio,‡ Lionel Perrin,*,‡ Pierre-Adrien Payard*,‡

Univ Lyon, UCBL, CNRS, ICBMS, UMR5246, ICBMS, 69622 Villeurbanne, France

Salt Effects, Oxidative Addition, Polymetallic Synergistic Effect, Palladium, DFT

Halide salts facilitate the oxidative addition of organic halides to Pd(0). This phenomenon originates from a combination of anionic, cationic and Pd-Pd cooperative effects. Exhaustive computational exploration at the DFT level of the complexes obtained from $[Pd^0(PPh_3)_2]$ and a salt (NMe_4Cl or LiCl) showed that chlorides promote phosphine release, leading to a mixture of mononuclear and dinuclear Pd(0) complexes. Anionic Pd(0) dinuclear complexes exhibit a cooperativity between Pd(0) centers which favors the oxidative addition of iodobenzene. The higher activity of Pd(0) dimers toward oxidative addition rationalizes the previously reported kinetic laws. In the presence of Li^+, the oxidative addition to mononuclear $[Pd^0L(Li_2Cl_2)]$ is estimated barrierless. LiCl coordination polarizes Pd(0), enlarging both the electrophilicity and the nucleophilicity of the complex, which promotes both coordination of the substrate and the subsequent insertion into the C-I bond. These conclusions are paving the way to the rational use of salt effect in catalysis for the activation of more challenging bonds.

Oxidative addition (OA) allows to access a variety of organometallic compounds through direct activation of organic electrophiles. It is the initiation step of many transition-metal-catalyzed reactions,[1] such as Pd-mediated cross-couplings.[2] In this context, it has been shown that the addition of halide salts such as LiCl, LiBr, LiI, Bu_4NI, Bu_4NF, $ZnCl_2$ can raise the yield of Pd-catalyzed cross-coupling of aryl triflate.[3, 4] The formation of anionic Pd(0) intermediates were suggested to account for these salt effect(s). The first mention of such anionic-Pd(0) salt is due to Negishi who described the generation of $[Pd^0(PPh_3)_2{\cdot}Li_2Cl_2]$ by the reduction of $[Pd^{II}Cl_2(PPh_3)_2]$ with an organolithium reagent (Scheme 1.a).[5] The activity of anionic Pd(0) complexes was explored in a series of seminal reports by Amatore and Jutand who studied the OA of aryl iodide to electrogenerated Pd(0) (Scheme 1.a).[6-10] Compared to the OA to $Pd^0(PPh_3)_2$, the OA of iodobenzene to electrogenerated Pd^0L_n in the presence of Cl^- or LiCl is much faster (Table 1).

Table 1. Salt effect on the oxidative addition of iodobenzene to Pd^0 in THF at 20°C.[6-10] Measured rate of oxidative addition k (L mol^{-1} s^{-1}) and variation of the activation energy ΔE_a (kcal mol^{-1}) with respect to the case of $Pd(PPh_3)_4$.

Proposed active complex (L = PPh_3)	k	ΔE_a
$[Pd^0L_2]$	16	0
$[Pd^0(PPh_3)_2Cl]^-$ or $[Pd^0(PPh_3)_2Cl]_2^{2-}$	530	-2.1
$[Pd^0(PPh_3)_n(LiCl)_m)]$	1320	-2.6

The electrogenerated mixture of anionic Pd(0) performs oxidative addition ca. 30 time faster than $Pd(PPh_3)_4$ (Table 1).[6] The kinetic law of this reaction features a second order with respect to Pd(0), pointing out the putative involvement of two Pd(0) centers in the rate determining step. The use of electrogenerated anionic Pd(0) also allowed to investigate cation effects on OA.[9] Further addition of Li^+ or Zn^{2+} salt allows to approximately triple the rate of OA compared to the anionic Pd(0) alone (Table 1).

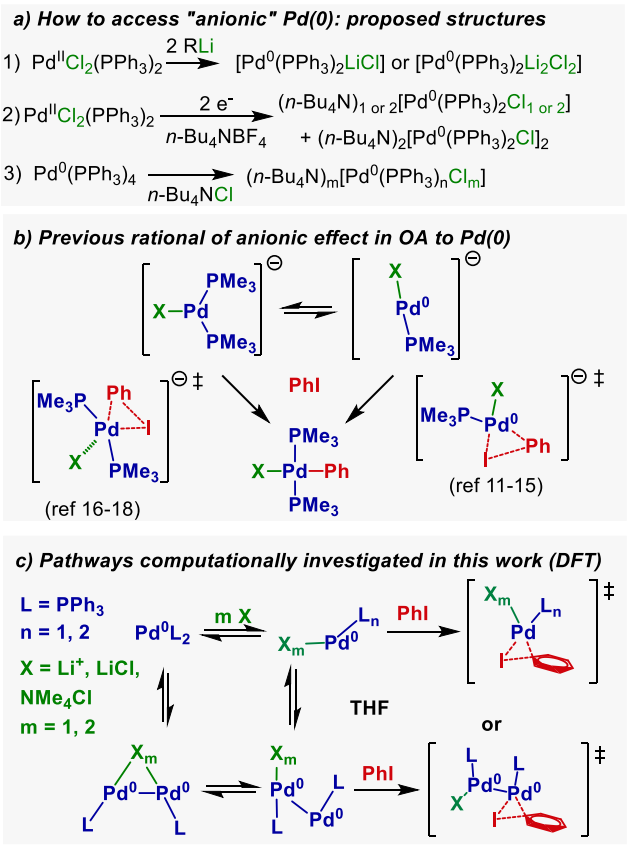

Scheme 1. a) Access to anionic Pd(0), b) previously suggested mechanisms for OA of aryl halides to anionic Pd(0) and c) strategy of the present work.

The molecular origin of this anionic effect is still the object of a lively debate (Scheme 1.b). The initially suggested pentacoordinate anionic Pd(0) intermediate[8] to account for the increased activity has been clearly excluded by DFT calculations.[11, 12] Currently, several scenari are still proposed. They either involve OA on a di-coordinated anionic complex $[(PMe_3)PdX]^-$,[11-15] or imply a charge effect due to the presence of X^- in the second coordination sphere of $Pd(PMe_3)_2$.[16-18] However, it is difficult to conclude as quantitative activation energies have not been yet computed for this chemical system using a realistic chemical model since most of the previous calculations were performed using PMe_3 as a model ligand and without the counter cation.[11-13, 16, 18]

Reviews by Mingos, Kurosawa and Zhao[19-21] offer a detailed overview of the structures and reactivity trends of Pd clusters. They enlighten the role played by dinuclear or trinuclear Pd complex in catalysis. As mentioned above, dinuclear Pd(0) complexes were suggested to favor OA based on kinetics data.[7, 22, 23] Though an OA mechanism involving cooperativity between two nitrogen-ligated Pd(0) was recently reported for OA,[24] anionic phosphine-ligated Pd(0) dimers were never considered to rationalize the higher activity of anionic Pd(0). Additionally, the role played by Li^+ alone or within LiCl on the overall kinetic effect is not documented. If Li^+ is not spectator, does it interact with iodine to assist C-I bond cleavage or indirectly promote OA by interacting with Pd or by electrostatic stabilization of the transition state (TS)? An in-depth comprehension of such polymetallic Pd/Pd and Pd/Li systems is needed and crucial to efficiently tune reactions in which a salt is added on purpose or produced *in situ* either from transmetalation or oxidative addition, or in the case of a supporting electrolyte or phase transfer agent (Scheme 1.a).

In this work computation are used to address: *i*) the theoretical level required to quantitatively compute the energetics of the system under study, *ii*) the nature and the aggregation state of the anionic Pd complexes formed, *iii*) the molecular origin of the anionic effect, *iv*) the evaluation of cooperative bi-metallic mechanisms, and *v*) the effect of the cation on the electronic properties of the complexes and on the mechanism. The speciation of Pd^0L_n complexes in solution, in absence and in presence of added is salts is discussed. In addition, the influence of added salts on the oxidative addition to anionic *vs* neutral most relevant Pd(0) complexes is discussed.

Computational Details

All DFT calculations were performed using the Gaussian 09 (Rev D.01) suite of programs.[25] Structure of minima and transition states were optimized using the M06 functional.[26] First to third period atoms (C, H, N, Li, P and Cl) were described using the double-ζ Karlsruhe basis set (def2-SVP).[27, 28] The fully relativistic ECP28MDF from the Stuttgart/Cologne group effective-core potential and its associated AVTZ basis set was used to describe Pd.[29] Iodine was described using the ECP46MWB quasi-relativistic effective-core potential[30] and its associated basis set augmented by a *d* polarization function $\alpha_{d(I)} = 0.730$.[31] Bulk solvent effects were taken into account using the SMD method as implemented in Gaussian.[32] The default cavity parameters, static and optical dielectric constants for THF were used. The anionic complexes were optimized with a counter cation to avoid overestimated the charge effects. The experimentally used ammonium cation *n*-Bu_4N^+ was modelled by Me_4N^+ for convenience. The impact of explicit THF coordination to Li^+ was investigated on the most favored pathways (Figure S24) and proved negligible as discussed below.

The nature of all stationary points was checked by analytical frequency calculations. Transition state (TS) connectivity was confirmed by computing the intrinsic reaction coordinate (IRC) in both directions. Harmonic frequencies were computed to estimate Gibbs free energies at 298 K under 1 atm pressure using the usual approximations. Natural Population Analysis and donor/acceptor second-order perturbation analysis was performed using NBO 6.[33] The Electron Localized Function (ELF) and condensed DFT functions analyses were performed using the Multiwfn package.[34]

To quantitatively account for the thermodynamic and kinetic features of the reaction, a benchmark against the experimental value of PdL_4 phosphine dissociation and iodobenzene OA to PdL_2 (see below) was performed and energies were further refined as follow. Gibbs free energies account for the change in standard states on going from the gas phase 1 atm state to the more relevant 1 mol L^{-1} solution state: $\Delta_rG_{1atm} \rightarrow \Delta_rG_{1M}$ = 1.89 kcal mol^{-1} for an associative pathway ($\Delta_r\nu$ = -1).[35] The Basis Set Superposition Error (BSSE) of either associative or dissociative pathways was corrected according to the counterpoise scheme.[36] Additionally, the entropy contribution was further corrected[37, 38, 39] for associative and dissociative steps. In our case, this correction accounts for +3.4 kcal mol^{-1} for a dissociative step. This set of corrections enables a fair match with both thermodynamic and kinetic experimental data. Both uncorrected and corrected energies are available in the SI (doc and XYZ).

Complexes are labelled using reduced formula: ^{Nx} is referring to the anionic Pd complexes neutralized by x ammonium NMe_4^+ counter cation(s) (1, 2), ^{Lix} is referring to the anionic complexes neutralized by x lithium counter cation(s) (1, 2, 3, 4). Adducts with iodobenzene will be noted •PhI, and transition states by ‡.

Results and discussion

The nature of $[Pd^0(PPh_3)_4]$ in THF was evaluated first to benchmark our computational method and to be used as a reference to understand the impact of added salt on phosphine dissociation and speciation.

Speciation of Pd^0L_n complexes in solution. Experimentally, in absence of additive, at millimolar concentration, $[Pd^0(PPh_3)_4]$ spontaneously dissociates one phosphine to form $[Pd^0(PPh_3)_3]$. The measured dissociation Gibbs free energy in toluene at 203 K is $\Delta_rG°_{exp}$(203 K) = +0.77 kcal mol^{-1}.[40] For comparison and benchmark purposes, the stability of each Pd complex upon successive phosphine dissociation has been computed relative to **PdL_4** taken as a reference (Table 2).The computed value of 2.1 kcal mol^{-1} to dissociate one phosphine from $[Pd^0(PPh_3)_4]$ offers a reasonable match with the experimental value of 0.77 kcal mol^{-1}.[40] This supports our computational model and level of theory. The speciation was then extended to Pd species mixed with the Me_4NCl salt. Experimentally, it was shown based on ^{31}P NMR analysis[24] that the electrochemical reduction of $Pd^0Cl_2(PPh_3)_2$ in the presence of the supporting electrolyte

(n-Bu)$_4$NNB$_4$ leads to the formation of at least three different anionic Pd(0) halide complexes in equilibria: (n-Bu$_4$N)$_{1\text{ or }2}$[Pd^0(PPh$_3$)$_2$Cl$_{1\text{ or }2}$] and (n-Bu$_4$N)$_2$[Pd^0(PPh$_3$)$_2$Cl]$_2$ were proposed (Scheme 1.a).[7, 16] To evaluate the relative stability of the complexes that could be formed under these conditions, one equivalent of **PdL$_2$** and NMe$_4$Cl were used as a reference to fit the experimental Pd/L ratio. Additionally, as the formation of **PdL$_3$** from **PdL$_2$** and **L** is exergonic by 9.5 kcal mol^{-1}, a sacrificial equivalent of **PdL$_2$** is added in the thermodynamic balance when **L** is released upon complex formation.

Table 2. Computed stability of **PdL$_n$** complexes relative to [Pd^0(PPh$_3$)$_4$] (PdL$_4$), Gibbs free energy ($\Delta_d G$, kcal mol^{-1}). Associated enthalpies and non-corrected free energies are available in Table S1.

Complex, label in parenthesis	$\Delta_d G$
[Pd^0(PPh$_3$)$_4$] (**PdL$_4$**)	0.0
[Pd^0(PPh$_3$)$_3$] (**PdL$_3$**) + PPh$_3$	2.1
[Pd^0(PPh$_3$)$_2$] (**PdL$_2$**) + 2 PPh$_3$	11.6
[Pd^0(PPh$_3$)] (**PdL**) + 3 PPh$_3$	33.8

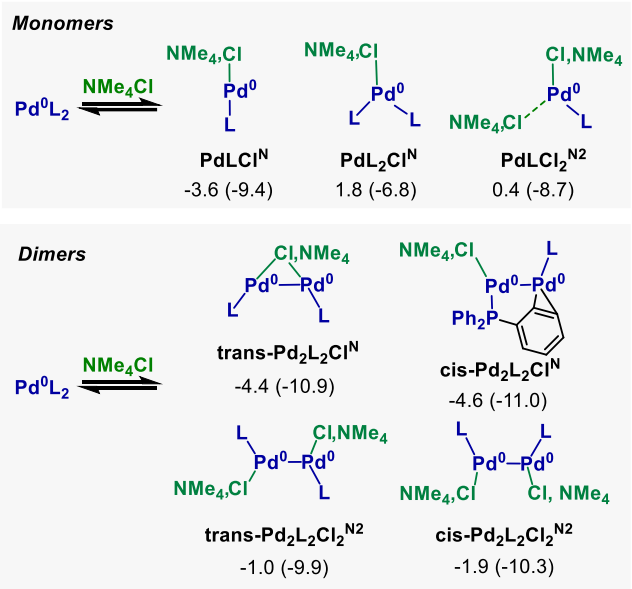

Scheme 2. Structures of Pd(0) monomers and dimers formed from a **PdL$_2$**/NMe$_4$Cl mixture. Computed disproportionation Gibbs free energies ($\Delta_d G$, kcal mol^{-1}) and enthalpies ($\Delta_d H$, kcal mol^{-1}, between parenthesis) *per* Pd are relative to **PdL$_2$** and x NMe$_4$Cl. Thermodynamics accounts for the capture of released L by a sacrificial equivalent of **PdL$_2$** to form **PdL$_3$**. Higher energy alternative structures (e.g. **PdL$_3$Cl^N** and **Pd$_2$L$_2$Cl$_2^{N2}$**) and associated enthalpies and non-corrected free energies are available in Table S2.

Based on computed thermodynamics (Scheme 2 and Table S2), the association of NMe$_4$Cl to PdL$_2$ to form the anionic complex NMe$_4$·[Pd^{0}L$_2$Cl] (**PdL$_2$Cl^N**, where ^{Nx} is referring to the x ammonium Me$_4$N$^+$ counter cation of the anionic complex, see the computational details) is endergonic by 1.8 kcal mol^{-1}, the formation of the dianionic complex proposed (NMe$_4$)$_2$·[PdL$_2$Cl$_2$] (**PdL$_2$Cl$_2^{N2}$**) is even more endergonic and not further considered. On the contrary, disproportionation to form the di-coordinated anionic complex NMe$_4$·[Pd^{0}LCl] (**PdLCl^N**) and **PdL$_3$** or the dissociated anionic and dianionic dimers NMe$_4$·[Pd$^0_2$L$_2$Cl] (**Pd$_2$L$_2$Cl^N**) and (NMe$_4$)$_2$·[Pd$^0_2$L$_2$Cl$_2$] (**Pd$_2$L$_2$Cl$_2^{N2}$**) and **PdL$_3$** are slightly exergonic by at least 1.0 kcal mol^{-1}. Since the energy of all these species are close, **PdL$_3$**, **PdLCl^N**, **Pd$_2$L$_2$Cl^N** and **Pd$_2$L$_2$Cl$_2^{N2}$** likely coexist as a mixture at ambient temperature. Their respective activity will be investigated and discussed in a following section.

Note that these equilibria are modified if anionic Pd(0) is not directly reduced *in situ* but rather generated by mixing a stable Pd(0) source, e.g. [Pd^0(PPh$_3$)$_4$], with a salt (Scheme 1.a). To mimic these conditions **PdL$_3$** and NMe$_4$Cl are taken as reference (Table S3) and released phosphine **L** is considered free in solution. The presence of Cl$^-$ favors phosphine dissociation compared to the case of **PdL$_3$** alone, but it remains the most chemically stable complex. However, under a large excess of chloride, the formation of **PdL$_2$Cl^N** (+6.0 kcal mol^{-1}), **PdLCl^N** (+6.5 kcal mol^{-1}) and **Pd$_2$L$_2$Cl^N** (+4.5 kcal mol^{-1}) become possible.

Cl is impacting the electronic structure of anionic Pd(0) complexes. In complex NMe$_4$·[Pd^{0}LCl] (**PdLCl^N**), the Cl atom mainly interacts through σ donation to Pd. The Natural Population Analysis (NPA) negative partial charge on Pd is increased to -0.38 compared to -0.33 in **PdL$_2$**. This results from the increase of the LUMO level from -0.92 eV (**PdL$_2$**) to -0.77 eV and of the HOMO level from -5.1 eV (**PdL$_2$**) to -4.78 eV (Figure S1). Complex **PdLCl^N** is thus more nucleophilic than **PdL$_2$**.

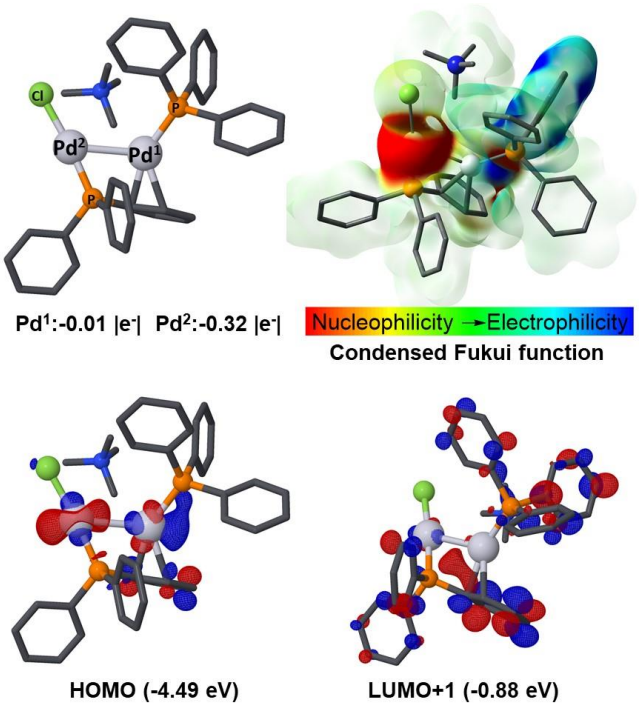

Figure 1. Structure, NPA charges, HOMO-LUMO plots and condensed Fukui function for **trans-Pd$_2$L$_2$Cl^N**.

Complex NMe$_4$.[Pd^{0}LCl] (**PdLCl^N**) can dimerize to form complexes NMe$_4$·[Pd$^0_2$L$_2$Cl] (**Pd$_2$L$_2$Cl^N**) and NMe$_4$.[Pd$^0_2$L$_2$Cl$_2$] (**Pd$_2$L$_2$Cl$_2^{N2}$**). Both feature a direct Pd-Pd bond as indicated by the existence of a Pd-Pd Electron Localized Function

(ELF) bond critical point, independently of the presence of a bridging chlorine atom (Figure S2-4). The electron density at the critical point is indicative of a weak metallophilic interaction (0.03 a.u. for **trans-Pd$_2$L$_2$Cl^N**).[41, 42] Complex NMe$_4$.[Pd$^0{}_2$L$_2$Cl] (**Pd$_2$L$_2$Cl^N**) has two isomers (Scheme 2). In the most stable one (**trans-Pd$_2$L$_2$Cl^N**), the two Pd centers are polarized as the low-lying energy LUMO+1 (-0.88 eV) is located on Pd^1, and the high-lying energy HOMO (-4.49 eV) is located on the other Pd^2 (Figure 1). This results in a substantial polarization of thePd$_2$ moiety, as indicated by the NPA charge difference of 0.31 |e$^-$| between the two atoms. Additionally, the decrease in the HOMO-LUMO gap of 0.44 eV relative to **PdLCl^N** reveals an enhanced polarizability of the complex.

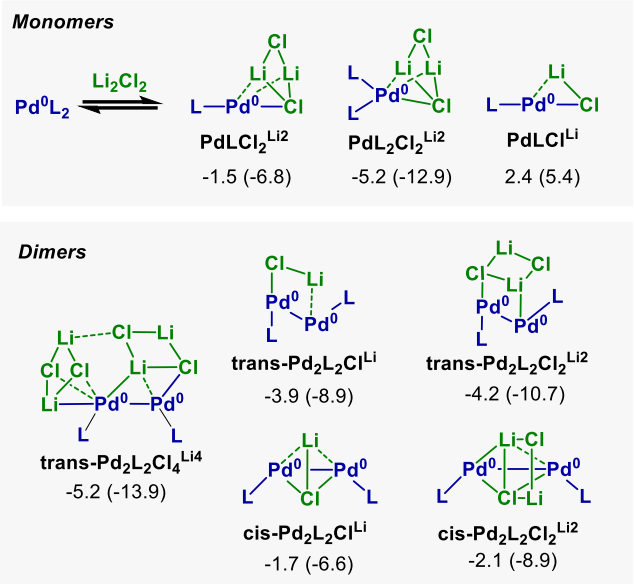

Scheme 3. Structures of Pd(0) monomers and dimers formed from a **PdL$_2$**/LiCl mixture. Computed disproportionation Gibbs free energies ($\Delta_d G$, kcal mol^{-1}) and enthalpies ($\Delta_d H$, kcal mol^{-1}, between parenthesis) *per* Pd are relative to **PdL$_2$** + x Li$_2$Cl$_2$. Thermodynamics accounts for the capture of released L by a sacrificial equivalent of **PdL$_2$** to form **PdL$_3$**. Higher energy alternative structures (e.g. **PdL$_2$Cl^{Li}**, **PdL$_3$Cl^{Li}** and **PdL$_3$Cl$_2$^{Li}** and **PdL$_2$Cl$_2$^{N2}**) and associated enthalpies and non-corrected free energies are available in Table S4.

The speciation of Pd complexes was then broadened to species that comprise lithium salt. The disproportionation free energy of the PdL$_2$/Li$_2$Cl$_2$ system were computed relative to **PdL$_2$** and Li$_2$Cl$_2$ as a reference (Scheme 3, Table S4). Coordination of the Li$_2$Cl$_2$ dimer to PdL$_2$ to yield [Li$_2$PdL$_2$Cl$_2$] (**PdL$_2$Cl$_2$^{Li2}**) is exergonic by 5.2 kcal mol^{-1} and favors the dissociation of one phosphine to form [LiPd^{0}LCl] (**PdLCl^{Li}**) and [Li$_2$Pd^{0}LCl$_2$] (**PdLCl$_2$^{Li2}**). As in the case of the ammonium countercation, dimerization to form complex **Pd$_2$L$_2$Cl^{Li}**, **Pd$_2$L$_2$Cl$_2$^{Li2}** and **Pd$_2$L$_2$Cl$_4$^{Li4}** is also exergonic by ca. 4 kcal mol^{-1}.

These dimer complexes all feature a weak Pd-Pd interaction as in the absence of Li$^+$ (Figures S5-10). We have previously shown that the chloride can bridge two Pd centers such as in **Pd$_2$L$_2$Cl^N** (Figure 1) but the presence of Li also enables another structure in which the Pd-Pd-Cl-Li core displays a four-membered ring as in **Pd$_2$L$_2$Cl^{Li}** (Figure 2). Such a structure displays some similarities with other systems in which interaction between Ni(0) and a Li has been described.[43, 44] In **Pd$_2$L$_2$Cl^{Li}**, **Pd$_2$L$_2$Cl$_2$^{Li2}** and **Pd$_2$L$_2$Cl$_4$^{Li4}** the Pd-Pd is also highly polarized, displaying partial charges like in **Pd$_2$L$_2$Cl^N** but on the overall both Pd centers are more electron poor than in **Pd$_2$L$_2$Cl^N** (Figure 2). This results in a particularly low-lying energy LUMO at -1.15 eV located on the Pd^1 ligated to Li and a HOMO delocalized on the Pd^2 bonded to Cl (Figure 2). The energy of the HOMO is similar to the one computed in the monomeric anionic Pd complex **PdLCl^N** (ca. -4.7 eV).

The most stable monomer **PdLCl$_2$^{Li2}** share a common feature with the Pd(0) dimers described above. The HOMO of this complex is centered on the Pd while the low lying LUMO (-1.00 eV) is localized between Pd and Li (Figure S11). As for the above-described Pd(0) dimers, the presence of salt lowers the HOMO-LUMO gap and shifts their location enhancing the polarity and polarizablity.

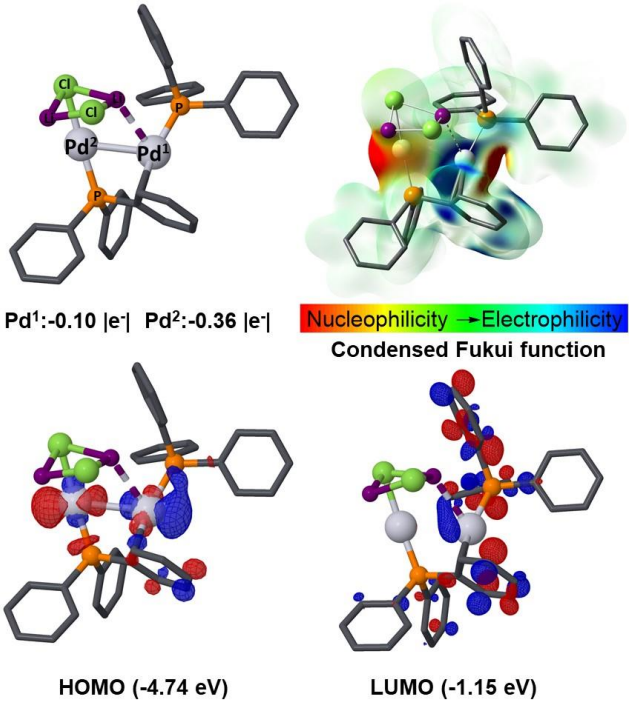

Figure 2. Structure, NPA charges, HOMO-LUMO plots and condensed Fukui function for the Pd-Pd non-bridged Pd-Pd (A) and Pd-Pd bridged (B) isomer structures of **Pd$_2$L$_2$Cl^{Li}**.

The expected formation of Pd(0)-dimers and of a variety of Pd(0) anionic complexes in equilibrium in the presence of NMe$_4$Cl (Scheme 2) or LiCl (Scheme 3) contrasts with the hypothesis made in previous computational studies dedicated to anion effect on OA to Pd.[11-18] The analysis of the electronic structure of the most stable complexes has evidenced the salt-induced polarization of the electronic density. Pd(0) dimers features non-equivalent Pd-centers: one nucleophilic and the other one electrophilic. LiCl impacts the electronic structure of mononuclear Pd(0) complexes in a similar way.

OA to monomeric anionic vs neutral Pd complexes. Experimentally, the kinetics of the oxidative addition of PhI to Pd^0(PPh$_3$)$_3$ in THF features a negative first order with respect to PPh$_3$ and a positive first order with respect to Pd

and PhI. Based on this observation it was proposed that $Pd^0(PPh_3)_2$ would be the active form of Pd(0) toward oxidative addition.[45, 46] Computationally, starting from $Pd^0(PPh_3)_3$ (**PdL₃**), phosphine dissociation to form the nearly linear $Pd^0(PPh_3)_2$ (**PdL₂**) complex ([P-Pd-P] = 153°) is endergonic by 9.6 kcal mol^{-1} (Figure 3). The formation of the iodobenzene adduct with $Pd^0(PPh_3)_2$ **PdL₂•PhI** is also thermodynamically disfavored as indicated by an overall endergonicity of +10.6 kcal mol^{-1} relative to separated $Pd^0(PPh_3)_3$ and PhI. In terms of bonding, the elongation of the C-I bond from 2.10 in PhI to 2.17 Å in **PdL₂•PhI** results from the back-donation from *d*-orbital of Pd to the σ*-C-I orbital of PhI while the short Pd-C^{ipso}(Ph) bond of 2.16 Å results from the donation from the π-orbitals of PhI to the low lying *s* and *p* orbitals of **PdL₂**. From the adduct **PdL₂•PhI**, oxidative addition is taking place through a concerted insertion of Pd in the C-I bond as displayed by transition state **PdL₂PhI‡** (Figure 3, path i).

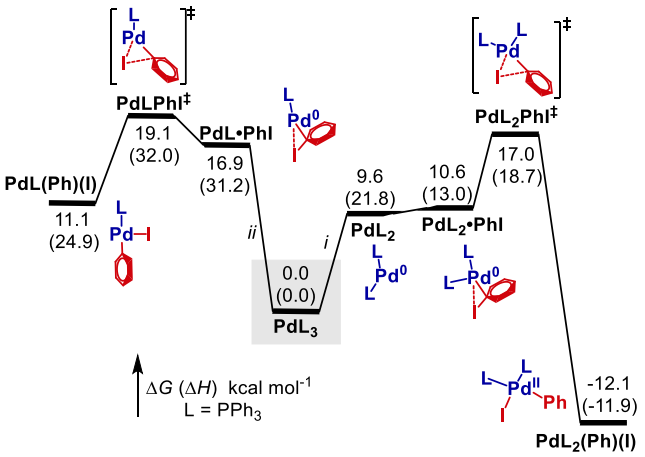

Figure 3. Gibbs free energy (Δ*G*, kcal mol^{-1}) and enthalpy shown in parentheses (Δ*H*, kcal mol^{-1}) pathways for the OA of PhI to $[Pd^0(PPh_3)_3]$ **PdL₃**; *i.* OA pathway to $Pd^0(PPh_3)_2$ (**PdL₂**); *ii.* OA pathway to $Pd^0(PPh_3)_3$ (**PdL₃**). Associated non-corrected enthalpies and free energies are available in the SI (Table S5).

Experimental enthalpies and entropies of activation were reported for the oxidative addition of PhI to $Pd(PPh_3)_3$ in THF ($\Delta G^{\ddagger}$(298 K) = 17.5 kcal mol^{-1}, $\Delta H^{\ddagger}$ = 18.4 kcal mol^{-1}, $\Delta S^{\ddagger}$ = 3.0 cal mol^{-1} K^{-1}).[45] These values are in excellent agreement with the calculated ones ($\Delta G^{\ddagger}$(298 K) = 17.0 kcal mol^{-1}, $\Delta H^{\ddagger}$ = 18.7 kcal mol^{-1}, $\Delta S^{\ddagger}$ = 5.7 cal mol^{-1} K^{-1}). The bonding picture and the associated energy profile (Figures 3 and S12) thus fit with the experimental kinetic law and activation parameters.[45, 46] However, to demonstrate that this pathway is operative, an alternative one involving $Pd^0(PPh_3)$ was computed. It is energetically less favored than the $Pd^0(PPh_3)_2$ pathway (Figure 3, path ii). The **PdL₂** pathway will be used as a gauge in the subsequent section to assess salt effects on the reactivity of Pd complexes.

As previously mentioned, low valent Pd(0) "Pd^0L_2" in the presence of a salt can form so-called anionic-Pd(0) complexes. Firstly, we will present the reactivity of the anionic Pd monomer complexes NMe_4·$[Pd^0LCl]$ (**PdLCl^N**) and NMe_4·$[Pd^0L_2Cl]$ (**PdL₂Cl^N**) as they are both thermodynamically accessible (Scheme 2). The activity of these two complexes will be compared to the one of the *bis*-ligated $[Pd^0(PPh_3)_2]$ (**PdL₂**) complex. Both **PdLCl^N** (Figures 4 and S13) and **PdL₂Cl^N** (Figure S14) display lower binding affinities towards PhI of +6.0 and +4.3 kcal mol^{-1} respectively, compared to +1.0 kcal mol^{-1} for **PdL₂**. This is consistent with the lower percentage of donation from PhI to Pd in **PdLCl^N•PhI** 54% *vs* 59% in **PdL₂•PhI** (based on 2nd order interaction energies as evaluated by NBO analysis). This electronic trend is also visible in the structure of the PhI adducts. In **PdLCl^N•PhI** the C-I bond is slightly longer by 0.03 Å compared to the one in the neutral **PdL₂•PhI** complex. This originates from a higher back-donation from Pd to PhI while the Pd-C bond distance is shorter in **PdLCl^N•PhI** by 0.07 Å compared to the same neutral complex **PdL₂•PhI**.

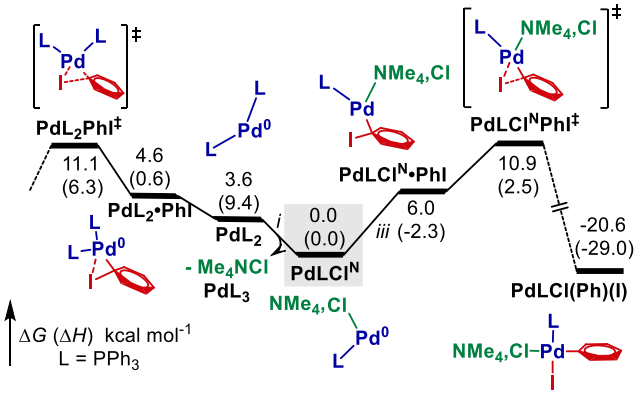

Figure 4. Gibbs free energy (Δ*G*, kcal mol^{-1}) and enthalpy shown in parentheses (Δ*H*, kcal mol^{-1}) pathways for the OA of PhI to monomeric anionic Pd(0) species, $NMe_4[Pd^0L_2Cl]$ (**PdLCl^N**) was used as an energy reference; *i.* OA to $[Pd^0L_2]$ (**PdL₂**); *iii.* OA pathway to $NMe_4[Pd^0LCl]$ (**PdLCl^N**). Associated non-corrected enthalpies and free energies are available in the SI (Table S6). Alternative pathways starting from **PdL₂Cl^N** (Figure S14) **PdLCl₂^{N2}** (FigureS15) and **PdL₂Cl₂^{N2}** (Figure S16) are available in the SI.

In the case of **PdLCl^N**, the lower affinity of PhI towards Pd is partially compensated by its higher ability to perform the oxidative addition as shown by the difference of energy between the oxidative addition transition state and PhI adduct (Figure 4): 4.9 kcal mol^{-1} for **PdLCl^N** *vs* 6.5 kcal mol^{-1} for **PdL₂**. The analysis of the geometries of **PdLCl^N•PhI** and **PdLCl^N•PhI‡** (Figure S13) reveals that the C-I bond distance is elongated from 2.20 to 2.30 Å, the Pd-I bond distance is shortened from 3.49 to 2.90 Å and the Pd-C bond length is elongated from 2.09 to 2.11 Å. In comparison, in absence of Me_4NCl, going from **PdL₂•PhI** to **PdL₂•PhI‡**, bond lengths of C-I is increased from 2.17 to 2.33 Å; the Pd-I one from 3.36 to 2.78 Å; and the Pd-C from 2.16 to 2.13 Å. This geometry trend betrays the higher ability of the anionic complex to transfer electron density to the electrophile and subsequently ease the OA step though the binding of the substrate is less favorable than in the PdL_2 pathway. Overall, an energy barrier of 10.9 kcal mol^{-1} is computed for **PdLCl^N**, a value that is comparable to the one of 11.1 kcal mol^{-1} computed for **PdL₂**. Finally, the TS of the OA to tricoordinate complex **PdL₂Cl^N** is much higher in energy at 16.5 kcal mol^{-1} (Figure S14).

To summarize this section, the energy barrier of OA to anionic Pd(0) monomer complexes, *i.e.* in presence of ammonium chloride salt, is similar to the one computed for $[Pd^0(PPh_3)_2]$ (Figure 4). This apparently contradicts the

assumption of the enhanced activity of anionic Pd complexes due to their putative higher nucleophilicities. As evidence above, this is not the case, as electron rich Pd unfavorably binds the electrophile. Actually, neutral **PdL$_2$** is slightly more active than anionic **PdL$_2$Cl^N**.[15] The higher activity observed experimentally for anionic complexes mainly originates from the reduction step performed in the absence of added phosphine. This contrasts with previously reported computational mechanistic studies[18] that assumed anionic Pd(0) to be more nucleophilic and thus more active. The lowest activity of monomeric anionic Pd(0) complexes is further supported by additional kinetic data from Amatore and Jutand collected on the OA of PhI to Pd^0(PPh$_3$)$_4$ in the presence of excess of NBu$_4$Cl. Under these conditions, OA is first order with respect with Pd(0), thus excluding the formation of dimers. The experimental free energy, enthalpies and entropies of activation in THF are $\Delta G^{\ddagger}$(298 K) = 18.7 kcal mol^{-1}, $\Delta H^{\ddagger}$ = 22.7 kcal mol^{-1}, $\Delta S^{\ddagger}$ = +13.4 cal mol^{-1} K^{-1}, all larger than in the case of Pd^0(PPh$_3$)$_4$ alone, as quoted above. Starting from PdL$_4$ and NMe$_4$Cl (Table S8), OA is mediated by **PdLCl^N** with overall activation free energy $\Delta G^{\ddagger}$ = 17.4 kcal mol^{-1}, $\Delta H^{\ddagger}$ = 22.1 kcal mol^{-1} and entropy $\Delta S^{\ddagger}$ = +15.8 cal mol^{-1} K^{-1}. This additional quantitative agreement between computed and experimental activation energies further reinforces our confidence in the modelling approach and in the species sampled. To conclude, both experimental and calculated values are indicative that the so-called "anionic effect" is primarily due to an easily accessible di-coordinated Pd(0).

OA to anionic Pd(0) dimers. Mechanisms based on mononuclear-Pd cannot account for the second order with respect to Pd reported by Amatore *et al* for electrogenerated anionic Pd(0).[6] In such a case, two Pd centers must be involved in the OA step. We have thus explored the reactivity of the Pd(0) dimer complexes NMe$_4$·[Pd$^0_2$L$_2$Cl] (**Pd$_2$L$_2$Cl^N**) and (NMe$_4$)$_2$·[Pd$^0_2$L$_2$Cl$_2$] (**Pd$_2$L$_2$Cl$_2^{N}$**) whose formation was computed to be exergonic when only two equiv of **L** *per* Pd are used (Scheme 2). Dimer complex **trans-Pd$_2$L$_2$Cl^N** is more active towards OA than monomer species (Figure 5). PhI coordinate to the neutral Pd(0) center (Figure 1) where the LUMO is mainly developed. The two Pd centers are transferring electron density to PhI (+0.12 |e$^-$| and +0.06 |e$^-$| respectively). The coordination to the other Pd center is possible but less favorable by c.a. 14 kcal mol^{-1} (Figure S17). De-coordination of the PPh$_3$ phenyl ring is required to enable the binding of PhI to the most electrophilic Pd(0). This results in an overall lower affinity of PhI to **Pd$_2$L$_2$Cl^N** compared to **PdL$_2$** and similar to the one of **PdLCl^N**. However, it is compensated in the case of anionic dimer complex by its higher ability to undergo C-I oxidative addition (3.6 kcal mol^{-1} *vs* 6.4 in **PdL$_2$•PhI**). This leads to an overall activation energy of 9.8 kcal mol^{-1}, *i.e.* 2.3 kcal mol^{-1} less than for **PdL$_2$** (Figure 5). The cooperation between the two Pd(0) allows to have an electrophilic Pd(0) center dedicated to the coordination step while the presence of the nucleophilic [Pd-Cl] moiety facilitates the addition step as already noticed for the mononuclear complexes.

Based on this kinetically favorable energy profile, we have considered the OA of a second PhI to the complex **Pd$_2$L$_2$Cl^N(Ph)(I)** yielded by the first OA (Figure S18). The second OA has an activation free energy of 22.8 kcal mol^{-1}. This is due to the highly unfavored coordination of PhI to the second electron rich Pd(0) center (+21.2 kcal mol^{-1}). Thereof, performing two successive OA on the dimer complex **Pd$_2$L$_2$Cl^N** is unlikely.

To highlight the influence of the charge of the complex on OA pathways, we have also explored the reactivity of the dianionic dimer complex (NMe$_4$)$_2$.[Pd$^0_2$L$_2$Cl$_2$] (**Pd$_2$L$_2$Cl$_2^{N2}$**) whose formation was computed to be exergonic by 1.9 kcal mol^{-1}. The binding of PhI to the Pd^1 center of **Pd$_2$L$_2$Cl$_2^{N2}$** requires the displacement of one chlorine atom from the first to the second coordination sphere of the complex. As a result, the binding energy is computed endergonic by +9.7 kcal mol^{-1} relative to separated **Pd$_2$L$_2$Cl$_2^{N2}$** and PhI (Figure S19). The energy barrier of OA relative to the energy of PhI adduct is decreased from 3.6 kcal mol^{-1} for the mono anionic system to 2.3 kcal mol^{-1} for the dianionic one. However, overall, this complex is less active with a global activation energy of 12.1 kcal mol^{-1}.

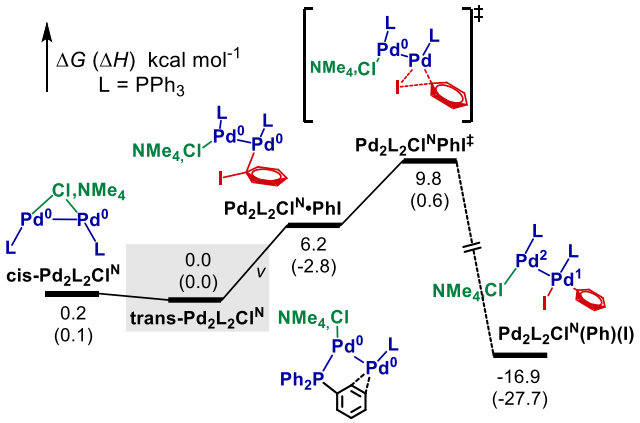

Figure 5. Gibbs free energy (ΔG, kcal mol^{-1}) and enthalpy shown in parentheses (ΔH, kcal mol^{-1}) pathways for the OA of PhI to anionic dimeric Pd(0) species, NMe$_4$[Pd$^0_2$L$_2$Cl] (**Pd$_2$L$_2$Cl^N**) was used as an energy reference; *v*. OA pathway to (NMe$_4$)[Pd$^0_2$L$_2$Cl] (**Pd$_2$L$_2$Cl^N**). Associated non-corrected enthalpies and free energies are available in the SI (Table S11). Alternative pathways starting from **Pd$_2$L$_2$Cl^N** (Figure S17) and **Pd$_2$L$_2$Cl$_2^{N2}$** (Figure S19) are available in the SI.

To summarize this section, the overall energy barriers for PhI OA to anionic Pd(0) dimers **Pd$_2$L$_2$Cl^N** and **Pd$_2$L$_2$Cl$_2^{N2}$** are around 6 kcal mol^{-1} lower in energy than the one computed for **PdL$_3$**. This trend originates from the compensation of the less favorable electrophile binding energy by the favorable thermodynamics of dimers formation and the reduced energy barrier for OA transition state relative to PhI adduct (kinetic contribution). This mechanism accounts for the second order relative to Pd determined by experimental kinetic studies and complements previous mechanistic pictures that were attributing the higher activity anionic Pd to putative higher nucleophilicity.

Effect of the Li-cation. As mentioned in the introduction, in the presence of both Li and Cl ions, electrogenerated Pd(0) show an even higher activity for oxidative addition than the one obtained in the sole presence of Cl and quaternary ammonium ions (Table 1). Indeed, is the overall kinetic effect only due to Li or to the LiCl combination? If so, does Li interacts with iodine to assist C-I bond cleavage or indirectly promote OA via the polarization of Pd as documented in the speciation section? The effect of Li$^+$ alone was

first explored by considering the hypothetical cationic $[Pd(0)\text{-}Li]^+$ complex. While such species are most unlikely to be formed in the presence of Cl^-, they are a straightforward model to estimate the magnitude of the cationic effect on OA.

As expected coordination of PhI to the cationic complex $[(PPh_3)PdLi]^+$ is highly favored (Figures S20-21, -15.2 kcal mol^{-1}). This fits the overall trend that iodobenzene coordination is favored on more electrophilic Pd(0). This is clearly evidenced by the linear correlation between global electrophilicity index (gie)[47] and association free energy (Figure S31) performed on all complexes considered in the present work. The adduct **[PdL^{Li}•PhI]$^+$** features a Li^+ cation chelated between Pd and the phenyl ring. No structure featuring Li-I interaction could be optimized either in the adduct or in the TS. However, there is an ion/induced-dipole interaction between Li^+ and Pd as evidenced by ELF analysis (Figure S22). Remarkably, though the electronic demand of **[PdL^{Li}]$^+$** and **PdLCl^N** systems are opposite, the energy barriers are identical for these two systems. OA requires 4.9 kcal mol^{-1} to proceed *i.e.* 1.5 kcal mol^{-1} less than from **PdL$_2$•PhI**. As indicated by the condensed Fukui function, in this system Li^+ acts as an electron acceptor – with the Ph ring of the electrophile – and the Pd as an electron donor interacting with the C-I bond. This once again highlights the cooperativity within metal centers as a key factor in mediating OA, here between Pd and Li, and in between two Pd as discussed above.

Effect of the LiCl salt. To decipher the structure of the electrogenerated Pd(0) complex that is the most favorable for the OA in the presence of LiCl, we have first studied the reactivity of monomer complexes $Li_2Pd^0LCl_2$ (**PdLCl$_2^{Li2}$**), $LiPd_0LCl$ (**PdLCl^{Li}**) and $Li_2Pd^0L_2Cl_2$ (**PdL$_2$Cl$_2^{Li2}$**) whose formation were computed to be exergonic (Scheme 3). In the profile displayed in Figure 6 (see Figure S23 for additional analysis), the energy of **PdLCl$_2^{Li2}$** and free PhI is taken as a reference point though the PhI adduct **PdLCl$_2^{Li2}$•PhI** is slightly more stable. Interestingly, **PdLCl$_2^{Li2}$** shows a higher binding affinity towards PhI (-1.1 kcal mol^{-1}) than does **PdL$_2$** (1.0 kcal mol^{-1}) due to its higher electrophilicity originating from the salt polarization as discussed in the speciation section. Kinetically, from the most stable adduct **PdLCl$_2^{Li2}$•PhI** the OA of PhI to the monomer complex **PdLCl$_2^{Li2}$** requires to overcome an overall energy barrier of 1.9 kcal mol^{-1}, the reaction is almost barrierless compared to the 9.0 kcal mol^{-1} computed for the **PdL$_2$** pathway (Figure 6). The additional stabilization observed, relative to the ammonium anionic complexes, originates either from the interaction of the phenyl ring with Li^+ or from the interaction with the I, the later path being slightly higher in energy by +0.4 kcal mol^{-1} (Figure 6). The impact of THF coordination to the Li centers of **PdLCl$_2^{Li2}$** on the OA energy barrier was evaluated using a microsolvatation model with one or two THF (Figure S24). While THF coordination is favoring the path featuring Li-I interaction, it has very little impact on the activation energy (0.4 to 1.4 kcal mol^{-1}).

The exploration of the reactivity of Pd(0) complexes in presence of LiCl was expanded to dimer Pd(0) complexes $[Pd_2L_2(LiCl)]$ (**Pd$_2$L$_2$Cl^{Li}**) and $[Pd_2L_2(LiCl)_2]$ (**Pd$_2$L$_2$Cl$_2^{Li2}$**) whose formation is exergonic as described in the speciation section (Scheme 3). Complexes **Pd$_2$L$_2$Cl^{Li}** and **Pd$_2$L$_2$Cl$_2^{Li2}$** have a high affinity for PhI as indicated by the computed binding energies of 2.6 and 1.8 kcal mol^{-1} respectively. This originates from non-symmetrical structure of the dimer complex in which LiCl or Li_2Cl_2 polarizes the two Pd atoms and enhances their global electrophilicities (Figure 2) as detailed in the speciation section. Relative to adducts **Pd$_2$L$_2$Cl^{Li}•PhI** or **Pd$_2$L$_2$Cl$_2^{Li2}$•PhI**, OA of PhI to the most electrophilic Pd center requires respectively 2.6 and 1.8 kcal mol^{-1}. Relative to separated PhI and **Pd$_2$L$_2$Cl^{Li}** or **Pd$_2$L$_2$Cl$_2^{Li2}$**, OA energy barrier have been computed to 6.1 and 5.8 kcal mol^1 (Figures S28-30). In the presence of Li^+, dimers are thus slightly less active than mononuclear Pd complexes in contrast to the case of Me_4N^+ (see previous section). This result once again agrees with the experimental results since no second order was reported in the case of added LiCl.[9]

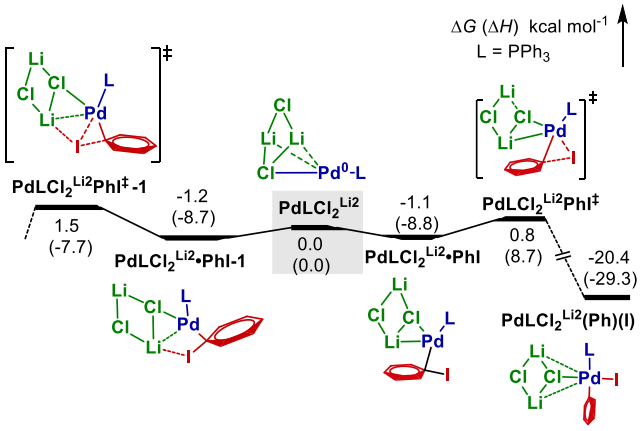

Figure 6. Gibbs free energy (ΔG, kcal mol^{-1}) and enthalpy shown in parentheses (ΔH, kcal mol^{-1}) pathways for the OA of PhI to monomeric **PdLCl$_2^{Li2}$**. Energy of **PdLCl$_2^{Li2}$** is used as a reference for the profile. **PdL$_2$** pathway *i)* is given for comparison. Associated non-corrected enthalpies and free energies are available in the SI (Table S16). Alternative pathways starting from **PdLCl$_2^{Li2}$**, **PdLCl$_2^{Li2}$(THF)** and **PdLCl$_2^{Li2}$(THF)$_2$** (Figure S24), **PdL$_2$Cl$_2^{Li2}$** (Figure S25), **PdLCl^{Li}** (Figure S26) and **PdL$_2$Cl^{Li}** (Figure S27) are available in the SI.

To summarize this section, the energy barrier for OA of PhI to monomeric Pd(0) complexes in the presence LiCl and two equivalents of **L** is decreased by up to 15 kcal mol^{-1} compared to **PdL$_3$**. This important effect is enabled by the monomer complex **PdLCl$_2$Li$_2$** in which Li and Cl synergistically and respectively promote the binding of the electrophile and the subsequent oxidative addition. This result and its interpretation are consistent with the experimental results (Table 1). This picture regarding the complementary effects of Li and Cl complements the preliminary interpretation of the anionic effect formulated by Norrby and co-workers who suggested a that Pd merely acts as a carrier of electron density from a nucleophilic to an electrophilic species.[15]

Conclusion: How to make a super-palladium?

The detailed computational investigation on the speciation of Pd(0) complexes in absence or presence of salts such as NMe_4Cl or LiCl reveals that a large set of mononuclear and dimer complexes can be formed. These complexes cover a diversity of electronic properties and bonding ability. The systematic investigation of their reactivity towards OA provides guidelines to use salt effects to tune the

catalytic properties of Pd(0) and provides some general trends in salts effects in organometallic chemistry.

The anions Cl^- mainly bind Pd via σ-donation which results in an increased negative charge on Pd that favors phosphine dissociation relative to the neutral Pd(0) complex. The stabilization of di-ligated Pd(0) intermediate is the first reason of the salt effect on the OA to Pd(0) (around 6 kcal mol^{-1}). After phosphine dissociation, both monomeric and dimeric mono or dianionic $(Pd_2L_2Cl_{1or2})^{-1\ or\ -2}$ complexes are thermodynamically accessible. The OA process is taking place in two steps, *i*) coordination of PhI and *ii*) insertion for Pd(0) into the C-I bond. The general trend for all complexes is that the more electron-deficient the Pd(0) center is that coordination of PhI occurs preferentially to the more electron-deficient Pd(0) center. Thus, PhI coordination to "anionic" Pd(0) is endergonic by 3 to 8 kcal mol^{-1}. In the case of anionic Pd(0) dimers this effect is partially balanced by the electrophilicity of the second Pd. Regarding mononuclear complexes, the interaction with LiCl increases their nucleophilicity (Cl) and electrophilicity (Li) enabling the exergonic PhI coordination of 3 kcal mol^{-1} in the most favorable case.

Finally, once the adduct formed, the insertion step is the most subtle to tune. Both electron rich complex **PdLCl^N** and electron poor one [**PdL^{Li}**]$^+$ are performing well. Looking only at the series of anionic monomers and dimers in the absence of Li^+, the overall trend is that the more electron rich Pd(0) the easier the insertion into the C-I bond. However, when Li is present within the complexes, no clear trend with electronic descriptors could be found. This is in line with the frontier orbital analysis of OA. Pd is inserting in the C-I bond through both donation from the π-system of PhI and backdonation in the σ* (C-I) orbital. Thus making Pd(0) either more nucleophilic or more electrophilic compared to PdL_2 favors OA kinetics. Overall the most active complexes are the ones which are both more electrophilic and more nucleophilic due to either i) cooperativity between Pd(0) centers or ii) Li^+, Cl^- synergistic effect. In both cases the electron giving and accepting areas of the Pd complexes are separated making up a "super-palladium": both more nucleophilic *and* more electrophilic. This interpretation at the molecular scale of salt effect in organometallic catalysis by which nucleophilic and electrophilic properties are enhanced by adequately located charged groups paves the way for further mechanistic understanding of salt effect in organometallic chemistry.

ASSOCIATED CONTENT

Supporting Information. Additional energy profiles and detailed orbitals and electron density analyses are provided (doc). Cartesian coordinates of all the optimized structures and their associated uncorrected (XYZ) and corrected (doc) energies are provided.

AUTHOR INFORMATION

Corresponding Author

*lionel.perrin@univ-lyon1.fr; pierre-adrien.payard@univ-lyon1.fr

ACKNOWLEDGMENT

This paper is dedicated to Prof. C. Amatore and Dr. A. Jutand, whose work is an endless source of inspiration and emulation for present and future generations of chemists.
The authors would like to thank Prof. O. Eisenstein, Dr. L. Grimaud, Dr. L. A. Perego and Dr. J. Vantourout for fruitful discussions. H. L. thanks the Chinese Scholarship Council (CSC) for a fellowship. The authors are grateful to the CNRS, ICBMS (UMR 5246), Université Lyon 1 and the Region Auvergne Rhone Alpes for financial support. The CCIR of ICBMS, PSMN and GENCI (allocation A10, A0100812501) are acknowledged for a generous allocation of computational resources and providing technical support.

REFERENCES

(1) Collman, J. P.; Roper, W. R., Oxidative-Addition Reactions of d8 Complexes. In *Advances in Organometallic Chemistry*, Stone, F. G. A.; West, R., Eds. Academic Press: 1969; Vol. 7, pp 53-94.
(2) *Handbook of Organopalladium Chemistry for Organic Synthesis*. Wiley: New York, 2003.
(3) Scott, W. J.; Stille, J. K., Palladium-catalyzed coupling of vinyl triflates with organostannanes. Synthetic and mechanistic studies. *J. Am. Chem. Soc.* **1986,** *108* (11), 3033-3040.
(4) Arcadi, A.; Cacchi, S.; Marinelli, F.; Morera, E.; Ortar, G., ß-aryl and ß-vinyl-αß-didehydro-α-aminoacid derivatives through the palladium-catalysed reaction of aryl and vinyl triflates with methyl α-acetamidoacrylate. *Tetrahedron* **1990,** *46* (20), 7151-7164.
(5) Negishi, E.-i.; Takahashi, T.; Akiyoshi, K., 'Bis(triphenylphosphine)palladium:' its generation, characterization, and reactions. *J. Chem. Soc. Chem. Commun.* **1986**, 1338-1339.
(6) Amatore, C.; Azzabi, M.; Jutand, A., Stabilization of bis(triphenylphosphine)palladium(0) by chloride ions. Electrochemical generation of highly reactive zerovalent palladium complexes. *J. Organometallic Chem.* **1989,** *363* (3), C41-C45.
(7) Amatore, C.; Azzabi, M.; Jutand, A., Role and effects of halide ions on the rates and mechanisms of oxidative addition of iodobenzene to low-ligated zerovalent palladium complexes $Pd^0(PPh_3)_2$. *J. Am. Chem. Soc.* **1991,** *113* (22), 8375-8384.
(8) Amatore, C.; Jutand, A.; Suarez, A., Intimate mechanism of oxidative addition to zerovalent palladium complexes in the presence of halide ions and its relevance to the mechanism of palladium-catalyzed nucleophilic substitutions. *J. Am. Chem. Soc.* **1993,** *115* (21), 9531-9541.
(9) Amatore, C.; Jutand, A., Mechanistic and kinetic studies of palladium catalytic systems. *J. Organometallic Chem.* **1999,** *576* (1), 254-278.
(10) Amatore, C.; Jutand, A., Anionic Pd(0) and Pd(II) Intermediates in Palladium-Catalyzed Heck and Cross-Coupling Reactions. *Acc. Chem. Res.* **2000,** *33* (5), 314-321.
(11) Gooßen, L. J.; Koley, D.; Hermann, H.; Thiel, W., The mechanism of the oxidative addition of aryl halides to Pd-catalysts: a DFT investigation. *Chem. Commun.* **2004**, 2141-2143.
(12) Goossen, L. J.; Koley, D.; Hermann, H. L.; Thiel, W., Mechanistic Pathways for Oxidative Addition of Aryl Halides to Palladium(0) Complexes: A DFT Study. *Organometallics* **2005,** *24* (10), 2398-2410.
(13) Goossen, L. J.; Koley, D.; Hermann, H. L.; Thiel, W., Palladium Monophosphine Intermediates in Catalytic Cross-Coupling Reactions: A DFT Study. *Organometallics* **2006,** *25* (1), 54-67.
(14) Ahlquist, M.; Norrby, P.-O., Oxidative Addition of Aryl Chlorides to Monoligated Palladium(0): A DFT-SCRF Study. *Organometallics* **2007,** *26* (3), 550-553.

(15) Ahlquist, M.; Fristrup, P.; Tanner, D.; Norrby, P.-O., Theoretical Evidence for Low-Ligated Palladium(0): [Pd−L] as the Active Species in Oxidative Addition Reactions. *Organometallics* **2006,** *25* (8), 2066-2073.
(16) Kozuch, S.; Shaik, S.; Jutand, A.; Amatore, C., Active Anionic Zero-Valent Palladium Catalysts: Characterization by Density Functional Calculations. *Chem. Eur. J.* **2004,** *10* (12), 3072-3080.
(17) Joy, J.; Stuyver, T.; Shaik, S., Oriented External Electric Fields and Ionic Additives Elicit Catalysis and Mechanistic Crossover in Oxidative Addition Reactions. *J. Am. Chem. Soc.* **2020,** *142* (8), 3836-3850.
(18) Kozuch, S.; Amatore, C.; Jutand, A.; Shaik, S., What Makes for a Good Catalytic Cycle? A Theoretical Study of the Role of an Anionic Palladium(0) Complex in the Cross-Coupling of an Aryl Halide with an Anionic Nucleophile. *Organometallics* **2005,** *24* (10), 2319-2330.
(19) Murahashi, T.; Kurosawa, H., Organopalladium complexes containing palladium-palladium bonds. *Coord. Chem. Rev.* **2002,** *231* (1), 207-228.
(20) Liu, Q.; Zhao, L., Low Valent Palladium Clusters: Synthesis, Structures and Catalytic Applications. *Chin. J. Chem.* **2020,** *38* (12), 1897-1908.
(21) Burrows, A. D.; Michael, D.; Mingos, P., Palladium cluster compounds. *Transit. Met. Chem.* **1993,** *18* (2), 129-148.
(22) Fumiyuki, O.; Akihiko, K.; Tamio, H., Generation of Tertiary Phosphine-Coordinated Pd(0) Species from $Pd(OAc)_2$ in the Catalytic Heck Reaction. *Chem. Lett.* **1992,** *21* (11), 2177-2180.
(23) Amatore, C.; Jutand, A.; Thuilliez, A., Formation of Palladium(0) Complexes from $Pd(OAc)_2$ and a Bidentate Phosphine Ligand (dppp) and Their Reactivity in Oxidative Addition. *Organometallics* **2001,** *20* (15), 3241-3249.
(24) Perego, L. A.; Payard, P.-A.; Haddou, B.; Ciofini, I.; Grimaud, L., Evidence for a Cooperative Mechanism Involving Two Palladium(0) Centers in the Oxidative Addition of Iodoarenes. *Chem. Eur. J.* **2018,** *24* (9), 2192-2199.
(25) Gaussian 09, Revision D.01, M. J. Frisch, G. W. Trucks, H. B. Schlegel, G. E. Scuseria, M. A. Robb, J. R. Cheeseman, G. Scalmani, V. Barone, B. Mennucci, G. A. Petersson, H. Nakatsuji, M. Caricato, X. Li, H. P. Hratchian, A. F. Izmaylov, J. Bloino, G. Zheng, J. L. Sonnenberg, M. Hada, M. Ehara, K. Toyota, R. Fukuda, J. Hasegawa, M. Ishida, T. Nakajima, Y. Honda, O. Kitao, H. Nakai, T. Vreven, J. A. Montgomery, Jr., J. E. Peralta, F. Ogliaro, M. Bearpark, J. J. Heyd, E. Brothers, K. N. Kudin, V. N. Staroverov, T. Keith, R. Kobayashi, J. Normand, K. Raghavachari, A. Rendell, J. C. Burant, S. S. Iyengar, J. Tomasi, M. Cossi, N. Rega, J. M. Millam, M. Klene, J. E. Knox, J. B. Cross, V. Bakken, C. Adamo, J. Jaramillo, R. Gomperts, R. E. Stratmann, O. Yazyev, A. J. Austin, R. Cammi, C. Pomelli, J. W. Ochterski, R. L. Martin, K. Morokuma, V. G. Zakrzewski, G. A. Voth, P. Salvador, J. J. Dannenberg, S. Dapprich, A. D. Daniels, O. Farkas, J. B. Foresman, J. V. Ortiz, J. Cioslowski, and D. J. Fox, Gaussian, Inc., Wallingford CT, 2013.
(26) Zhao, Y.; Truhlar, D. G., The M06 suite of density functionals for main group thermochemistry, thermochemical kinetics, noncovalent interactions, excited states, and transition elements: two new functionals and systematic testing of four M06-class functionals and 12 other functionals. *Theor. Chem. Acc.* **2008,** *120* (1), 215-241.
(27) Weigend, F.; Ahlrichs, R., Balanced basis sets of split valence, triple zeta valence and quadruple zeta valence quality for H to Rn: Design and assessment of accuracy. *Phys. Chem. Chem. Phys.* **2005,** *7* (18), 3297-3305.
(28) Weigend, F., Accurate Coulomb-fitting basis sets for H to Rn. *Phys. Chem. Chem. Phys.* **2006,** *8* (9), 1057-1065.
(29) Peterson, K. A.; Figgen, D.; Dolg, M.; Stoll, H., Energy-consistent relativistic pseudopotentials and correlation consistent basis sets for the 4d elements Y–Pd. *J. Chem. Phys.* **2007,** *126* (12), 124101.
(30) Bergner, A.; Dolg, M.; Küchle, W.; Stoll, H.; Preuß, H., Ab initio energy-adjusted pseudopotentials for elements of groups 13–17. *Mol. Phys.* **1993,** *80* (6), 1431-1441.
(31) Maron, L.; Teichteil, C., On the accuracy of averaged relativistic shape-consistent pseudopotentials. *Chem. Phys.* **1998,** *237* (1), 105-122.
(32) Marenich, A. V.; Cramer, C. J.; Truhlar, D. G., Universal Solvation Model Based on Solute Electron Density and on a Continuum Model of the Solvent Defined by the Bulk Dielectric Constant and Atomic Surface Tensions. *J. Phys. Chem. B* **2009,** *113* (18), 6378-6396.
(33) NBO 6.0. E. D. Glendening, J. K. Badenhoop, A. E. Reed, J. E. Carpenter, J. A. Bohmann, C. M. Morales, C. R. Landis, and F. Weinhold, Theoretical Chemistry Institute, University of Wisconsin, Madison (2013).
(34) Lu, T.; Chen, F., Multiwfn: A multifunctional wavefunction analyzer. *J. Comput. Chem.* **2012,** *33* (5), 580-592.
(35) Kelly, C. P.; Cramer, C. J.; Truhlar, D. G., Aqueous Solvation Free Energies of Ions and Ion−Water Clusters Based on an Accurate Value for the Absolute Aqueous Solvation Free Energy of the Proton. *J. Phys. Chem. B* **2006,** *110* (32), 16066-16081.
(36) Sparta, M.; Jensen, V. R.; Børve, K. J., Accurate metal–ligand bond energies in the η^2-C_2H_4 and η^2-C_{60} complexes of $Pt(PH_3)_2$, with application to their Bis(triphenylphosphine) analogues. *Mol. Phys.* **2013,** *111* (9-11), 1599-1611.
(37) Martin, R. L.; Hay, P. J.; Pratt, L. R., Hydrolysis of Ferric Ion in Water and Conformational Equilibrium. *J. Phys. Chem. A* **1998,** *102* (20), 3565-3573.
(38) Sieffert, N.; Bühl, M., Noncovalent Interactions in a Transition-Metal Triphenylphosphine Complex: a Density Functional Case Study. *Inorg. Chem.* **2009,** *48* (11), 4622-4624.
(39) Harvey, J. N.; Himo, F.; Maseras, F.; Perrin, L., Scope and Challenge of Computational Methods for Studying Mechanism and Reactivity in Homogeneous Catalysis. *ACS Catal.* **2019,** *9* (8), 6803-6813.
(40) Mann, B. E.; Musco, A., Phosphorous-31 Nuclear Magnetic-Resonance Spectroscopic Characterization of Tertiary Phosphine Palladium(0) Complexes - Evidence for 14-Electron Complexes in Solution. *J. Chem. Soc. Dalton Trans.* **1975**, 10.1039/dt9750001673 (16-1), 1673-1677.
(41) Lepetit, C.; Fau, P.; Fajerwerg, K.; Kahn, M. L.; Silvi, B., Topological analysis of the metal-metal bond: A tutorial review. *Coord. Chem. Rev.* **2017,** *345*, 150-181.
(42) Sculfort, S.; Braunstein, P., Intramolecular d^{10}–d^{10} interactions in heterometallic clusters of the transition metals. *Chem. Soc. Rev.* **2011,** *40* (5), 2741-2760.
(43) Borys, A.; Hevia, E., The Anionic Pathway in Nickel-Catalysed Cross-Coupling of Aryl Ethers. *Angew. Chem. Int. ed.* **2021,** *60*, 24659-24667.
(44) Nattmann, L.; Lutz, S.; Ortsack, P.; Goddard, R.; Cornella, J., A Highly Reduced Ni–Li–Olefin Complex for Catalytic Kumada–Corriu Cross-Couplings. *J. Am. Chem. Soc.* **2018,** *140* (42), 13628-13633.
(45) Fauvarque, J.-F.; Pflüger, F.; Troupel, M., Kinetics of oxidative addition of zerovalent palladium to aromatic iodides. *J. Organometallic Chem.* **1981,** *208* (3), 419-427.
(46) Amatore, C.; Pfluger, F., Mechanism of oxidative addition of palladium(0) with aromatic iodides in toluene, monitored at ultramicroelectrodes. *Organometallics* **1990,** *9* (8), 2276-2282.
(47) Parr, R. G.; Pearson, R. G., Absolute hardness: companion parameter to absolute electronegativity. *J. Am. Chem. Soc.* **1983,** *105* (26), 7512-7516.

Oxidative Addition: How to Become a "Super-Palladium"